Impact Comminution of Solids Due to Progressive Crack Growth Driven by Kinetic Energy of High-Rate Shear

Zdeněk P. Bažant[1]
McCormick Institute Professor and
W.P. Murphy Professor of Civil Engineering
and Materials Science
Northwestern University,
2145 Sheridan Road,
CEE/A135,
Evanston, IL 60208
e-mail: z-bazant@northwestern.edu

Yewang Su[1]
Research Assistant Professor
Department of Civil and
Environmental Engineering,
Northwestern University,
Evanston, IL 60208;
State Key Laboratory of Nonlinear Mechanics,
Institute of Mechanics,
Chinese Academy of Sciences,
Beijing 100190, China
e-mail: yewangsu@imech.ac.cn

A new theory, inspired by analogy with turbulence, was recently proposed to model the apparent dynamic overstress due to the energy that is dissipated by material comminution during penetration of missiles into concrete walls. The high-rate interface fracture comminuting the material to small particles was considered to be driven by the release of kinetic energy of high-rate shear of the forming particles, and the corresponding energy dissipation rate was characterized in the damage constitutive law by additional viscosity. However, in spite of greatly improved predictions for missile impact and penetration, the calculation of viscosity involved two simplifications—one crude simplification in the calculation of viscosity from the shear strain rate, and another debatable simplification in treating the comminution as an instantaneous event, as in the classical rate-independent fracture mechanics. Presented is a refined theory in which both simplifications are avoided without making the theory significantly more complicated. The interface fracture is considered to be progressive and advance according to Evans' power law extended to the fast growth of interface crack area. The growth rate of interface cracks naturally leads to an additional viscosity, which allows close matching of the published test data. In combination with the microplane damage constitutive model M7 for concrete, the refined theory gives a close match of the exit velocities of missiles penetrating concrete walls of different thicknesses and of the penetration depths of missiles of different velocities into a massive block. [DOI: 10.1115/1.4029636]

Keywords: missile impact, penetration, fragmentation of concrete, dynamic fracture, crack growth rate, viscous damping, particle size distribution, turbulence, finite element analysis, dynamic overstress

1 Introduction

The understanding and prediction of dynamic fracture and comminution of materials is important for missile of meteorite impact, ground shock, explosions, mining, fracturing of gas or oil shale, and various industrial processes. Vast literature exists [e.g., 1–24] but it need not be reviewed here in detail since a review was provided in a recent paper [25].

One major difficulty at high-rate fracture has, for many years, been the phenomenon of apparent "dynamic overstress," This means that the material strength or energy dissipation at strain rates $\gg 1$/s apparently increases by order of magnitude above the value predicted by statically measured strength and the quasi-static rate effects due to bond ruptures at crack tips and viscoelasticity of material between the cracks. Many attempts for numerical simulation of dynamic overstress under missile impact on concrete or rock have been made. But despite the use of the most realistic damage constitutive model, such as the microplane model, the deceleration of penetrating missile was severely underestimated. The data could be fitted only with a large ad hoc, physically unexplained, increase of either the damping or the strength limits of the material [2], by which, of course, predictability in new situations and the experimental basis in uni-, bi-, and tri-axial material tests with postpeak damage have been forfeited.

A caveat must here be mentioned. Commercial codes, such as ABAQUS, automatically insert artificial damping both in the solver and the finite elements. This generates a bulk viscosity pressure that is linear or quadratic in the volumetric strain rate. The user is often unaware of it and some such measures are not even clear from the manual. It is important to check for such artificial damping. Properly, one should eliminate all such artificial damping from the commercial program and use only physically justified damping or viscosity. Introduction of sufficiently strong artificial damping can largely or totally obviate the problem of dynamic overstress. This is probably the reason why some authors have recently claimed that the missile impact data can be reproduced numerically with no additional viscosity, but apparently they have not checked whether different choices of damping might be needed to fit very different situations. Similar comments apply to the ad hoc artificial choice of elevated strength limits in the microplane model [2].

The reason for insufficiency of the quasi-static damage constitutive models obviously is that they account only for the degree of fragmentation seen in static laboratory tests by which they are calibrated. In these static tests, the size of the smallest fragments is roughly 1/3 of the maximum aggregate size in concrete. But under impact, much smaller particles are generated. This is what must lead to a great increase of energy dissipation or apparent viscosity.

Although the micromechanics of dynamic comminution, which includes the propagation and branching of cracks, their interference with waves, and the interaction of a few cracks, has been well understood for some time [1], a work attempting to develop a

[1]Corresponding authors.

Contributed by the Applied Mechanics Division of ASME for publication in the JOURNAL OF APPLIED MECHANICS. Manuscript received December 20, 2014; final manuscript received January 15, 2015; published online February 11, 2015. Editor: Yonggang Huang.

constitutive model that could be used in large finite element codes for predicting the impact and penetration of missiles into concrete or rock appeared only very recently [25–27].

In that recent work, a new idea was introduced into the dynamic analysis of high velocity impacts or powerful explosions—the dynamic comminution into fine particles under compression is caused not by the release of the strain energy, as in classical fracture mechanics, but by the release of the kinetic energy of high shear strain rate of particles that are about to form. Depending on the particle size, this kinetic energy can exceed the maximum possible value of the stored strain energy by orders of magnitude, and its analysis leads to a model partly analogous to turbulence.

In a preceding work [25,27], the latest version, M7, of the microplane model for concrete was enhanced by material viscosity calculated under two simplifying hypotheses:

(1) One, rather crude, simplification was that the additional shear viscosity was calculated so as to yield a dissipation rate proportional to the stress invariant of shear stress required to drive interface fracture. This simplification was admissible because that invariant had the dimension of energy per unit volume. But the value of the proportionality constant had to be left to data fitting, and the relationship of that invariant to energy dissipation and viscosity was only approximate, although very good fits of penetration data were obtained.
(2) The second hypothesis was that the interface fracture producing the comminuted particles occurs instantaneously.

In reality, the interface fracture must, of course, occur progressively. This is modeled here by a high-rate extension of Evans's power law for subcritical crack growth (although it remains debatable whether this approach properly reflects the simultaneity of crack growth at many interfaces). The apparent viscosity is then calculated from energy balance.

2 Local Kinetic Energy Density Due to Material Comminution

To simplify analysis, the comminution of a solid is assumed to produce identical hexagonal prisms with side $h/2$ and length h to be determined later (Fig. 1). The solid undergoes shear strain ϵ_{Dij} at the rate $\dot{\epsilon}_{Dij}$, as depicted by transition from Figs. 1(*a*) and 1(*b*) (the superior dot denotes derivative with respect to time t). At a certain moment, the effective deviatoric strain rate $\dot{\epsilon}_D = \sqrt{\dot{\epsilon}_{Dij}\dot{\epsilon}_{Dij}/2}$ becomes high enough for the local kinetic energy to suffice for creating interface shear fractures and slips that separate the particles. In this process, the kinetic energy of shear strain field gets converted into the interface fracture energy. This energy can be calculated as the difference between the kinetic energies per unit volume of the original solid before (Fig. 1(*b*)) and after (Fig. 1(*c*)) the comminution. This yields [25] the kinetic energy drop per unit volume of solid

$$-\Delta\mathcal{K} = c_k \rho h^2 \dot{\epsilon}_D^2 \tag{1}$$

where ρ is the mass density and $c_k = I_p/(2hV_p)$. Also, $I_p = 5\sqrt{3}h^4/128$ and $V_p = 3\sqrt{3}h^3/8$ are the polar moment of inertia and volume of each hexagonal prism, respectively. Usually $H/h = 10$–100 and $H = 1/10$ of the size of fragments that dominate in static crushing of the solid. An important point in derivation of Eq. (1) is that the kinetic energy of the strain rate field is separable from, and additive to, the kinetic energy of the global motion in the shear plane, defined by the velocities of particle centers [25].

In practice, the particle size is always randomly distributed over a certain range, $s \in [h, H]$, where h and H now denote the minimum and maximum particle sizes. An empirical distribution, the Schuhmann power law [28], well justified in mining literature [28–30], is considered. Accordingly, the volume fraction of particles of size $h < s$ is

$$F(s) = \frac{s^k - h^k}{H^k - h^k} \quad [s \in (h, H), F(s) \in (0, 1)] \tag{2}$$

where k is an empirical constant; $k \approx 0.5$. Assuming that energy contributions of particles of various sizes s can be superposed, the kinetic energy drop for particles of all sizes per unit volume of the original solid is thus obtained as

$$-\Delta\mathcal{K} = \int_{s=h}^{H} c_k \rho s^2 \dot{\epsilon}_D^2 \, \mathrm{d}F(s) = C_k \rho h^2 \dot{\epsilon}_D^2 \tag{3}$$

where $C_k = c_k k(r^{k+2} - 1)/\left[(k+2)(r^k - 1)\right]$ = dimensionless constant and $r = H/h$ [25]. For $H/h = 10$ and $k = 0.5$, $C_k = 1.5186$.

The interface area per unit volume of particles of size s can be calculated as c_s/s, where $c_s = 1 + 4/\sqrt{(3)}$ = dimensionless constant. For the particles distributed according to the Schuhmann law, the particle interface area per unit volume is

$$S = \int_{s=h}^{H} \frac{c_s}{s} \mathrm{d}F(s) = \frac{C_s}{h} \tag{4}$$

Here, $C_s = c_s k(r^{k-1} - 1)/\left[(k-1)(r^k - 1)\right]$ = dimensionless constant [25]. Here, it is assumed that $H/h = 10$ and then $k = 0.5$, $C_s = 1.0465$.

The type of behavior is decided by the dimensionless number

$$B_a = \frac{-\Delta\mathcal{K}}{\tau_0^2/(2G_s)} \tag{5}$$

which represents the ratio of the kinetic energy density of shear to the maximum possible strain energy density, the latter being $\tau_0^2/(2G_s)$ where τ_0 = shear strength and G_s = elastic shear modulus of the solid. Kinetic comminution must happen when $B_a \gg 1$

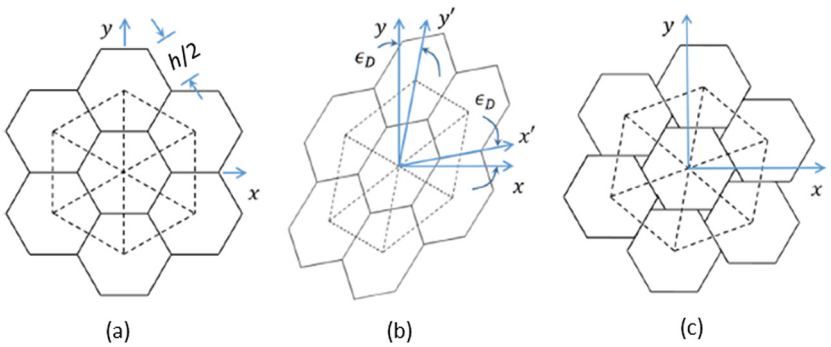

Fig. 1 Schematic illustration of material comminution into prismatic hexagonal particles: (*a*) undeformed state, (*b*) shearing regime, and (*c*) comminuted regime

and cannot happen when $B_a \ll 1$. For concrete, the transition occurs at $\dot{\epsilon}_D \approx 1/s$. The expression for B_a in terms of h, Γ, and ρ given in Refs. [25,26] is not exactly true here although the general definition in Eq. (5) is the same.

3 Continuous Evolution of Comminution According to Evans' Law for Static Crack Growth

Two theoretically possible forms of dynamic fracture criterion were considered in Ref. [25]. One, which was similar to the classical fracture mechanics, assumed that fracture occurs as soon as it is triggered by incremental energy balance, i.e., $-d\Delta\mathcal{K}/dS = \Gamma =$ interface fracture energy of the material. The other form assumed a total energy balance, $-\Delta\mathcal{K} = \Gamma S$, which seems more reasonable since, rather than propagating, the fracture occurs simultaneously at numerous interfaces (in a parallel study [31], the latter form is used with success to develop a more rigorous theory for viscous energy dissipation accounting more accurately for the work of comminution).

However, in both forms of fracture criterion a complete interface fracture of all particles was assumed to occur instantaneously. In reality, the interface fracture must evolve at a certain finite rate, even though that rate may be extremely high. It might, of course, be so high, compared to the strain rate, that the assumption of instantaneous fracture might be closer to the truth. A debatable point though this is, here we pursue the hypothesis that a gradual rather than instantaneous comminution fracture is more realistic.

Aside from the extended Evans' law of crack growth [32,33], which is adopted here for fast growth of interface fracture surface, some other kinetic equations of a similar form have been also proposed for dynamic crack growth. Particularly, Paliwal and Ramesh [34], based on the work by Freund [1] and Deng [35], introduced for fast crack growth rates the following general equation: $\dot{l} = c_{\max}[(K_I - K_{IC})/(K_I - K_{IC}/2)]^{\gamma}$. They applied it to the modeling of the damage evolution of brittle materials containing dilute wing cracks [34].

Even though Evans' has never been used for fast dynamic growth, it is nevertheless adopted here because it has a solid physical foundation. It was derived from Kramer's rule of transition rate theory [36] Eqs. (6)–(12) and [33] Eqs. (29)–(34) coupled with the activation energy concept. This derivation showed that Evans' law must not be limited to very slow rates but must also apply to very fast rates. According to this law,

$$\dot{S} = A_{Tk}\left(\frac{K}{K_c}\right)^n = A_T\left(\frac{\mathcal{G}}{\Gamma}\right)^{n/2} \tag{6}$$

$$\text{where} \quad A_T = Ae^{-Q_0/kT} \tag{7}$$

Here, K and K_c are stress intensity factor and its critical value (fracture toughness), $\mathcal{G}$ = energy release rate (with respect to S rather than time), n = empirical constant (typically about 10), A = material constant, Q_0 = activation energy of fracture growth, k = Boltzmann constant, and T = absolute temperature. As argued before, the total form of energy balance at interface crack formation appears to be more realistic than the incremental form, i.e., $S\mathcal{G} = -\Delta\mathcal{K}$. Thus, the rate of the interface fracture area becomes

$$\dot{S} = A_T\left(\frac{-\Delta\mathcal{K}}{\Gamma S}\right)^{n/2} \tag{8}$$

Substitution of Eqs. (3) and (4) into Eq. (8) gives the governing equation for the rate of interface area

$$\dot{S} = \frac{C_T}{S^{3n/2}}\left(\frac{\rho\dot{\epsilon}_D^2}{\Gamma}\right)^{n/2} \tag{9}$$

Here, $C_T = A_T(C_k C_s^2)^{n/2}$ is a constant. For numerical analysis, this differential equation needs to be converted to an incremental difference equation. To this end, the equation is integrated by separation of variables under the assumption that the strain rate, $\dot{\epsilon}_D$, is constant during time step $\Delta t = t_{new} - t_{old}$. The integration yields

$$S_{new} = \left[C_T\left(\frac{\rho\dot{\epsilon}_D^2}{\Gamma}\right)^{n/2} m\Delta t + S_{old}^m\right]^{1/m}, \quad m = 1 + \frac{3n}{2} \tag{10}$$

Here, S_{old} and S_{new} are the interface areas at the beginning and end of the time increment, respectively.

As proposed in Ref. [25], in computations the kinetic energy drop can be dissipated by the work of an additional stress, which is more convenient to implement than dissipation by an additional body force. Energy conservation requires that the work of additional stress be equal to the kinetic energy drop that is converted to the energy of new interface; i.e.,

$$\Gamma\Delta S = s_{ij}^A \Delta\epsilon_{Dij} \tag{11}$$

Here, $i, j = 1,2,3$; s_{ij}^A is the deviatoric stress tensor doing work on $\dot{\epsilon}_{Dij}$ during material comminution. The additional stress could also be represented as a viscous stress

$$s_{ij}^A = \eta_D \dot{\epsilon}_{Dij} \tag{12}$$

where η_D = viscosity. Equations (9), (11), and (12), together with the replacement of S by S_{new}, gives

$$\eta_D = C_T \frac{\rho^{n/2}}{2\Gamma^{n/2-1}} \frac{\dot{\epsilon}_D^{n-2}}{S_{new}^{3n/2}} \tag{13}$$

in which the interface area S_{new} is given by Eq. (10). The use of S_{new} instead of S_{old} represents a backward difference approximation, which requires iterations with repeated use of Eq. (10). The backward difference approximation is more stable than a forward or central difference approximation, in which S_{new} in Eq. (13) would be replaced by S_{old} or by $(S_{old} + S_{new})/2$.

If the particle size is of interest, it may be calculated for each location and each time step from Eq. (4), i.e., $h = C_s/S$. In the previous version of the theory [25] inspired by analogy with turbulence, a version in which the interface fracture was considered to occur instantaneously (as in classical fracture mechanics), it was found that

$$h \propto \dot{\epsilon}_D^{-2/3}, \quad \Delta\mathcal{K} \propto \dot{\epsilon}_D^2/3, \quad \eta_D\dot{\epsilon}_D^{-1/3} \tag{14}$$

where $\propto$ is the proportionality sign.

These simple relations have analogies in the theory of turbulence, the eddies being considered as analogous to the comminuted particles. The analogies can be detected in the eddy size, in the kinetic energy dissipation by viscous friction between the eddies, and in the effective viscosity. However, in the present theory with finite rate of interface fracture growth, these simple relations are not valid. Nevertheless, from the physical viewpoint, they should be approached asymptotically as S increases, because the fracture propagation criterion in linear elastic fracture mechanics is the limit case of Evans' law for $A_T \to \infty$.

4 Verification by Tests of Impact With Perforation or Partial Penetration of Concrete Walls

Circular slabs, made of concrete WES-5000 with mass density 2300 kg/m^3, were impacted by projectiles at the Geotechnical and Structural Laboratory of the U.S. Army Engineer Research and Development Center (ERDC), Vicksburg [9,37]. All the slabs were cast in steel culvert pipes with the diameter of 1.52 m. Their thicknesses were 127, 216, 254, and 280 mm. The impacting projectiles had a diameter of 50.8 mm, weighed 2.3 kg, had a

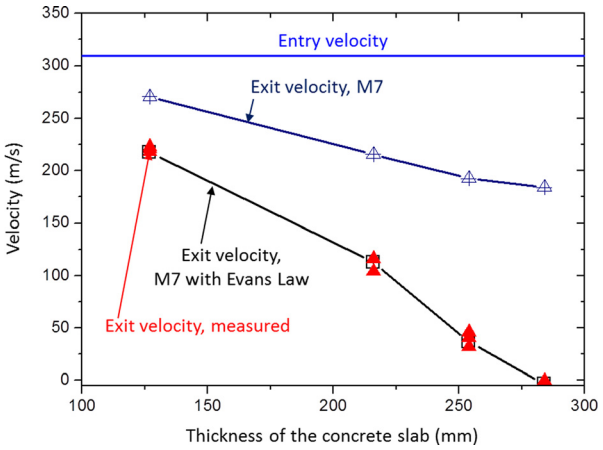

Fig. 2 Comparison of the exit velocity predicted by two methods (M7 with and without implementation of comminution effect) with the experimental data for missile perforation of concrete walls (the thicknesses of impacted walls range 127–280 mm)

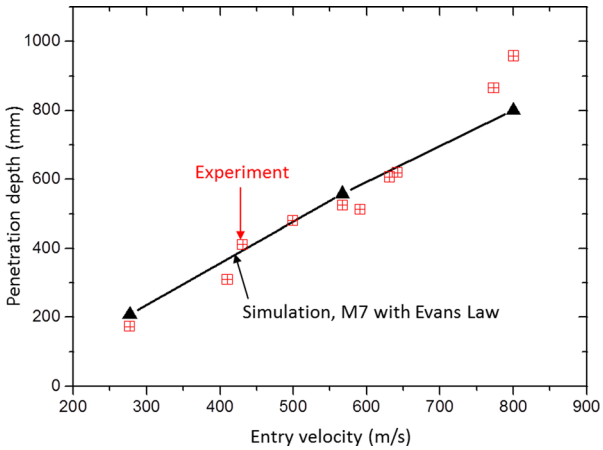

Fig. 3 Comparison of the penetration depth predicted by two methods (M7 with and without implementation of comminution effect) and the experimental data (the entry velocities of the missiles range from 277 m/s to 800 m/s)

hollow steel body with an ogival nose (caliber radius head = 3.0, length/diameter ratio = 7.0), and were considered as rigid since they were found undeformed after the test. They hit the concrete slab at the center, orthogonally (the impact angle of 90 deg), with the entry velocity of 310 m/s. For each slab thickness, the perforation was repeated two or three times. No damage was discerned on the projectiles after the tests.

As the damage constitutive law, microplane model M7 [38,39] was used. It was calibrated to reproduce the Young's modulus of $E = 25$ GPa, Poisson ratio $\nu = 0.18$, and the mean compressive strength of $\bar{f}_t = 48$ MPa, The M7 scaling parameters [39] were $k_1 = 11 \times 10^{-5}, k_2 = 110, k_3 = 30, k_4 = 100$, and $k_5 = 10^{-4}$. With these parameters, model M7 fits well all the basic types of static laboratory tests of uni-, bi-, and triaxial behavior with postpeak softening and size effect, as published in the literature, and the tests of WES-5000 concrete for various special loading paths [38,39].

Without the additional viscosity, the use of the calibrated microplane model M7 led to severe overestimation of the measured exit velocities (see the dashed curve in Fig. 2), as previously reported by Caner and Bažant [27]. However, with the present comminution theory, the measured velocities and penetration depths were matched closely. The optimum fits shown correspond to the interface fracture energy of $\Gamma = 100$ N/m, Evans' law exponent of $n = 3$, and prefactor $A_T = 2 \times 10^9$ m^2/s (it is interesting that this optimum value of n is much lower than the n-value for static crack growth, which is 10–20).

Energy absorbing elements were used in finite element computations at the slab perimeter, to avoid spurious rebound waves. The projectile was in the simulations and thus considered to be rigid. This was partly justified by the fact that no visually discernible damage to the projectile was found in the experiments. So the deformation of the projectile must have been elastic, but this is very small.

For $A_T = 2 \times 10^9$ m^2/s, the four predicted exit velocities agree with all the experimental data closely (Fig. 2). They also match the data better than the comminution simulations with simplified viscosity presented in Ref. [27]; see Fig. 2.

The tests of penetration depths used a slightly different concrete, the CSPC concrete [37], but it was so similar to the WES-5000 concrete that the same mechanical parameters, besides the adjustment of A_T, could be used. The concrete wall was big and thick enough to be considered as semi-infinite. The projective had an ogive nose, weighed 0.9 kg, and length of 242.4 mm and diameter of 25.9 mm. The entry velocities ranged from 277 m/s to 800 m/s.

As shown in Fig. 3, the penetration depth increases with the increase of the entry velocity. For $A_T = 5 \times 10^8$ m^2/s, Fig. 3 documents that the present comminution model can give excellent agreement with the observed penetration depths.

Finally it may be pointed out that, despite the strain softening in the constitutive model, there is, here, no need for nonlocal damage modeling with a material characteristic length. The reason is that the strain rate was so high that the inertia must have prevented the damage localization instability from taking place at the same rate and also so high that nonlocal damage interactions could not occur within time periods shorter than the time a sound wave would need to travel the material characteristic length.

5 Conclusions

(1) Extending the recently proposed idea [40] to model the dynamic overstress or enhanced resistance to missile penetration, explosion or shock wave transmission due to comminution of compressed material caused by the release of kinetic energy of high-rate shearing, this paper shows that the finiteness of the rate of interface crack growth can be taken into account using Evans' power law for subcritical crack growth.

(2) Based on Evans' law, the growth rate of interface crack area is considered as a function of the shear strain rate, current interface area, material density, and interface fracture energy.

(3) What is important for computations is to dissipate the energy of fracturing at the correct rate. This is easily achieved by incorporating into the damage constitutive model an additional shear viscosity, which is found to be a function of the current shear strain rate, total interface area between comminuted particles, fracture energy, and mass density.

(4) At the same time, any artificial damping automatically introduced in commercial finite element programs must be eliminated, both on the structural and element levels.

(5) This additional rate effect comes on top of the quasi-static rate effects due to the formation of macrocracks and to the viscoelasticity of material between the macrocracks, which are normally embedded in a quasi-static constitutive law such as microplane model M7. The additional rate effect asymptotically vanishes as the strain rate decreases (in practice, below about 1/s).

(6) The additional viscosity can be derived from energy balance, by equating the work of fracturing to the macro-dissipation of energy by viscosity.

(7) As a difference from previous theory, the additional viscosity is proportional not simply to the $-1/3$ power the strain rate, but to both the $n-2$ power of that rate and also to the $-3\ n/2$ power of the interface area, which itself depends on the strain rate history ($n =$ Evans' law exponent).
(8) Although the problem is highly nonlinear, it is possible to formulate an iterative explicit finite-element algorithm in which the interface area increments are calculated from the current total interface area and the average strain rate in the time step. The algorithm converges well and, with a supercomputer, delivers realistic results, as demonstrated for systems with millions of nodal displacements.
(9) Computer simulations in which the microplane constitutive damage model M7 is enriched with the present additional viscosity lead to excellent fits of published test data on the projecticle penetration of concrete walls of different thicknesses and on the depth of penetration of projectiles of different velocities into a large concrete block.
(10) The use of Arrhenius law for the Evans law prefactor should allow generalizations to variable temperature.
(11) In conjunction with the use of a realistic damage constitutive model such as microplane model M7, the high-rate simulations remain anchored in all the experimentally evidenced uni-, bi-, and triaxial damage properties postpeak softening (which, for M7, are characterized by 22 different types of quasi-static tests of concrete [39]).

Acknowledgment

The authors gratefully acknowledge the support from the U.S. Army Research Office, Durham, to Northwestern University, during the initial phase of research under Grant No. W911NF-09-1-0043/P00003. An additional support obtained from the ADD, Korea, through a Daejeon University grant to Northwestern University is also acknowledged. Thanks are due to Professor Ferhun Caner, Visiting Scholar on leave from UPC, Barcelona, for making available his coding of M7 and the meshes for slab perforations.

References

[1] Freund, L. B., 1998, *Dynamic Fracture Mechanics*, Cambridge University Press, New York.
[2] Adley, M. D., Frank, A. O., and Danielson, K. T., 2012, "The High-Rate Brittle Microplane Concrete Model: Part I: Bounding Curves and Quasi-Static Fit to Material Property Data," Comput. Concr., **9**(4), pp. 293–310.
[3] Cadoni, E., Labibes, K., Albertini, C., Berra, M., and Giangrasso, M., 2001, "Strain-Rate Effect on the Tensile Behaviour of Concrete at Different Relative Humidity Levels," Mater. Struct., **34**(1), pp. 21–26.
[4] Camacho, G., and Ortiz, M., 1996, "Computational Modelling of Impact Damage in Brittle Materials," Int. J. Solids Struct., **33**(20), pp. 2899–2938.
[5] Deshpande, V., and Evans, A., 2008, "Inelastic Deformation and Energy Dissipation in Ceramics: A Mechanism-Based Constitutive Model," J. Mech. Phys. Solids, **56**(10), pp. 3077–3100.
[6] Doyoyo, M., 2002, "A Theory of the Densification-Induced Fragmentation in Glasses and Ceramics Under Dynamic Compression," Int. J. Solids Struct., **39**(7), pp. 1833–1843.
[7] Ferri, E., Deshpande, V., and Evans, A., 2010, "The Dynamic Strength of a Representative Double Layer Prismatic Core: A Combined Experimental, Numerical, and Analytical Assessment," ASME J. Appl. Mech., **77**(6), p. 061011.
[8] Forquin, P., Gary, G., and Gatuingt, F., 2008, "A Testing Technique for Concrete Under Confinement at High Rates of Strain," Int. J. Impact Eng., **35**(6), pp. 425–446.
[9] Frank, A. O., Adley, M. D., Danielson, K. T., and McDevitt, H. S., Jr., 2012, "The High-Rate Brittle Microplane Concrete Model: Part II: Application to Projectile Perforation of Concrete Slabs," Comput. Concr., **9**(4), pp. 311–325.
[10] Gailly, B. A., and Espinosa, H. D., 2002, "Modelling of Failure Mode Transition in Ballistic Penetration With a Continuum Model Describing Microcracking and Flow of Pulverized Media," Int. J. Numer. Methods Eng., **54**(3), pp. 365–398.
[11] Gatuingt, F., and PijaudierCabot, G., 2002, "Coupled Damage and Plasticity Modelling in Transient Dynamic Analysis of Concrete," Int. J. Numer. Anal. Methods Geomech., **26**(1), pp. 1–24.
[12] Grady, D., 1982, "Local Inertial Effects in Dynamic Fragmentation," J. Appl. Phys., **53**(1), pp. 322–325.
[13] Grady, D., 1998, "Shock-Wave Compression of Brittle Solids," Mech. Mater., **29**(3–4), pp. 181–203.
[14] Grady, D., and Kipp, M., 1979, "The Micromechanics of Impact Fracture of Rock," Int. J. Rock Mech. Min. Sci. Geomech. Abstr., **16**(5), pp. 293–302.
[15] Grady, D., and Kipp, M., 1995, "Experimental Measurement of Dynamic Failure and Fragmentation Properties of Metals," Int. J. Solids Struct., **32**(17), pp. 2779–2791.
[16] Grady, D. E., 1990, "Particle Size Statistics in Dynamic Fragmentation," J. Appl. Phys., **68**(12), pp. 6099–6105.
[17] Hemmert, D. J., Smirnov, V. I., Awal, R., Lati, S., and Shetty, A., 2010, "Pulsed Power Generated Shockwaves in Liquids From Exploding Wires and Foils for Industrial Applications," 16th International Symposium on High Current Electronics (16th SHCE), Tomsk, Russia, Sept. 19–24, pp. 537–540.
[18] Kožar, I., and Ožbolt, J., 2010, "Some Aspects of Load-Rate Sensitivity in Visco-Elastic Microplane Material Model," Comput. Concrete, **7**(4), pp. 317–329.
[19] Mescall, J., and Weiss, V., eds., 1983, *Materials Behavior Under High Stress and Ultrahigh Loading Rates. Part II* (Sagamore Army Materials Research Conference Proceedings, Vol. 29), Plenum Press, New York.
[20] Maurel, O., Reess, T., Matallah, M., De Ferron, A., Chen, W., La Borderie, C., Pijaudier-Cabot, G., Jacques, A., and Rey-Bethbeder, F., 2010, "Electrohydraulic Shock Wave Generation as a Means to Increase Intrinsic Permeability of Mortar," Cem. Concr. Res., **40**(12), pp. 1631–1638.
[21] Mott, N., 1947, "Fragmentation of Shell Cases," Proc. R. Soc. London, Ser. A, **189**(1018), pp. 300–308.
[22] Obolt, J., Sharma, A., and Reinhardt, H.-W., 2011, "Dynamic Fracture of Concrete Compact Tension Specimen," Int. J. Solids Struct., **48**(10), pp. 1534–1543.
[23] Shih, C., Nesterenko, V., and Meyers, M., 1998, "High-Strain-Rate Deformation and Comminution of Silicon Carbide," J. Appl. Phys., **83**(9), pp. 4660–4671.
[24] Wei, Z., Evans, A., and Deshpande, V., 2009, "The Influence of Material Properties and Confinement on the Dynamic Penetration of Alumina by Hard Spheres," ASME J. Appl. Mech., **76**(5), p. 051305.
[25] Bažant, Z. P., and Caner, F. C., 2014, "Impact Comminution of Solids Due to Local Kinetic Energy of High Shear Strain Rate: I. Continuum Theory and Turbulence Analogy," J. Mech. Phys. Solids, **64**, pp. 223–235.
[26] Bažant, Z. P., and Caner, F. C., 2013, "Comminution of Solids Caused by Kinetic Energy of High Shear Strain Rate, With Implications for Impact, Shock, and Shale Fracturing," Proc. Natl. Acad. Sci., **110**(48), pp. 19291–19294.
[27] Caner, F. C., and Bažant, Z. P., 2014, "Impact Comminution of Solids Due to Local Kinetic Energy of High Shear Strain Rate: II. Microplane Model and Verification," J. Mech. Phys. Solids, **64**(1), pp. 236–248.
[28] Schuhmann, R., Jr., 1940, "Principles of Comminution, I—Size Distribution and Surface Calculations," American Institute of Mining, Metallurgical, and Petroleum Engineers, Englewood, CO, AIME Technical Publication No. 1189.
[29] Charles, R. J., 1957, "Energy-Size Reduction Relationships in Comminution," Trans. Am. Inst. Min. Metall. Eng., **208**(1), pp. 80–88.
[30] Ouchterlony, F., 2005, "The Swebrec Function: Linking Fragmentation by Blasting and Crushing," Min. Technol., **114**(1), pp. 29–44.
[31] Su, Y., Bažant, Z. P., Zhao, Y., Salviato, M., and Kedar, K., 2015, "Viscous Energy Dissipation of Kinetic Energy of Particles Comminuted by High-Rate Shearing Under Missile Impact," Int. J. Fract., (in press).
[32] Evans, A. G., 1972, "A Method for Evaluating the Time-Dependent Failure Characteristics of Brittle Materials—and Its Application to Polycrystalline Alumina," J. Mater. Sci., **7**(10), pp. 1137–1146.
[33] Le, J.-L., Bažant, Z. P., and Bazant, M. Z., 2011, "Unified Nano-Mechanics Based Probabilistic Theory of Quasibrittle and Brittle Structures: I. Strength, Static Crack Growth, Life Time and Scaling," J. Mech. Phys. Solids, **59**(7), pp. 1291–1321.
[34] Paliwal, B., and Ramesh, K. T., 2008, "An Interacting Micro-Crack Damage Model for Failure of Brittle Materials Under Compression," J. Mech. Phys. Solids, **56**(3), pp. 896–923.
[35] Deng, H., and Nemat-Nasser, S., 1992, "Dynamic Damage Evolution in Brittle Solids," Mech. Mater., **14**(2), pp. 83–104.
[36] Bažant, Z. P., Le, J.-L., and Bazant, M. Z., 2008, "Size Effect on Strength and Lifetime Distributions of Quasibrittle Structures Implied by Interatomic Bond Break Activation," 17th European Conference on Fracture (ECF-17), Brno, Czech Republic, Sept. 2–5, pp. 78–92.
[37] Cargile, J. D., 1999, "Development of a Constitutive Model for Numerical Simulation of Projectile Penetration into Brittle Geomaterials," U.S. Army Engineer Research and Development Center, Vicksburg, MS, Technical Report No. SL-99-11.
[38] Caner, F. C., and Bažant, Z. P., 2013, "Microplane Model M7 for Plain Concrete. I: Formulation," J. Eng. Mech., **139**(12), pp. 1714–1723.
[39] Caner, F. C., and Bažant, Z. P., 2012, "Microplane Model M7 for Plain Concrete. II: Calibration and Verification," J. Eng. Mech., **139**(12), pp. 1724–1735.
[40] Bažant, Z. P., and Caner, F. C., 2014, "Corrigendum to Impact Comminution of Solids Due to Local Kinetic Energy of High Shear Strain Rate: I. Continuum Theory and Turbulence Analogy [J. Mech. Phys. Solids 64 (2014) 223–235]," J. Mech. Phys. Solids **67**(1), p. 14.